# The $CO_2$ cycloaddition to epoxides and aziridines promoted by porphyrin-based catalysts

Caterina Damiano[a], Paolo Sonzini[a], Matteo Cavalleri[a], Gabriele Manca[b]* and Emma Gallo[a]*

[a]Department of Chemistry, University of Milan, Via C. Golgi 19, 20133 Milan (Italy). E-mail: emma.gallo@unimi.it.

[b]Istituto di Chimica dei Composti OrganoMetallici, ICCOM-CNR, Via Madonna del Piano 10, I-50019 Sesto Fiorentino (Italy). E-mail: gabriele.manca@iccom.cnr.it

## *Abstract*

Thanks to its intrinsic eco-compatibility and high atom economy, the direct insertion of $CO_2$ into three-membered rings, such as epoxides and aziridines, has become one of the most investigated strategies for the synthesis of cyclic carbonates and oxazolidin-2-ones. In this view, the following short account summarizes our recent results regarding the use of ruthenium porphyrin complexes and metal-free porphyrins, in combination with TBACl (tetrabutyl ammonium chloride), to promote the $CO_2$ conversion into cyclic carbonates as well as *N*-alkyl and *N*-aryl oxazolidin-2-ones. Experimental data are described in combination with performed DFT studies that allowed proposing a reaction mechanism for the $CO_2$ cycloaddition to aziridines promoted by metal-free porphyrins in which the adduct formed by **$TPPH_2$** and TBACl represents the real catalytic active species.

***Keywords****:* carbon dioxide, cyclic carbonates, oxazolidin-2-ones, porphyrins, catalysis, DFT studies

## 1. Introduction

The constant growth of greenhouse gases concentration in the atmosphere, responsible of global warming and air pollution, represents one of the major and more troubling problems of our society. For centuries the human activities have evolved and industrialized by producing massive quantities of gaseous wastes, especially carbon dioxide that now constitutes about three-quarter of the greenhouse gases. This worrisome situation has encouraged the scientific community to find new solutions and technologies capable to *reduce*, *recover* and *recycle* carbon dioxide. High efforts have been devoted in replacing fossil fuels with renewable and climate-friendly energy sources [1, 2] to reduce the $CO_2$ emissions and, complementarily, CCS (Carbon Capture and Storage) and CCU

(Carbon Capture and Utilization) [3] strategies have been developed to remove $CO_2$ from the atmosphere and reuse it as a C1 carbon source [4]. In fact, in view of its abundance, non-toxicity and low-cost, carbon dioxide should be considered, rather than an annoying waste, a valuable resource to produce fuels [5] and chemicals [6].

Even if $CO_2$ is an attractive starting material, the high stability and chemical inertness of this gas turns it into a very challenging substrate for the synthesis of fine chemicals. Therefore, competencies and energies have been invested in developing catalytic methodologies able to incorporate $CO_2$ into organic skeletons in order to produce compounds presenting a higher added value by applying eco-friendly procedures. Among all the organic reactions involving carbon dioxide, the $CO_2$ cycloaddition to three-membered ring compounds, such as epoxides and aziridines, has gained great attention and represents one of the most investigated strategies for the synthesis of cyclic carbonates [7-9] and oxazolidin-2-ones [10, 11]. The importance of developing efficient procedures for the $CO_2$ cycloaddition to three-membered rings lies in the intrinsic eco-compatibility of the process due to the 100% atom economy of the $CO_2$ utilization. In order to preserve this asset, the research has moved towards the use of non-toxic and easily-to-handle homogenous [12-14] and heterogeneous [15-21] catalytic systems, including metal complexes and organocatalysts, able to mediate the process under mild experimental conditions, such as low temperatures, low $CO_2$ pressures and low catalytic loadings. It is important to note that the $CO_2$ cycloaddition to three-membered rings needs the co-presence of electrophilic (E) and nucleophilic (Nu) species that, according to most accepted mechanism, are respectively in charge to activate and open the tensioned heterocycle for allowing the carbon dioxide insertion (scheme 1). Thus, efficient procedures require the use of binary catalytic systems formed by an electrophilic metal complex, or organocatalyst, and a nucleophilic agent, such as a quaternary ammonium salt or an organic base.

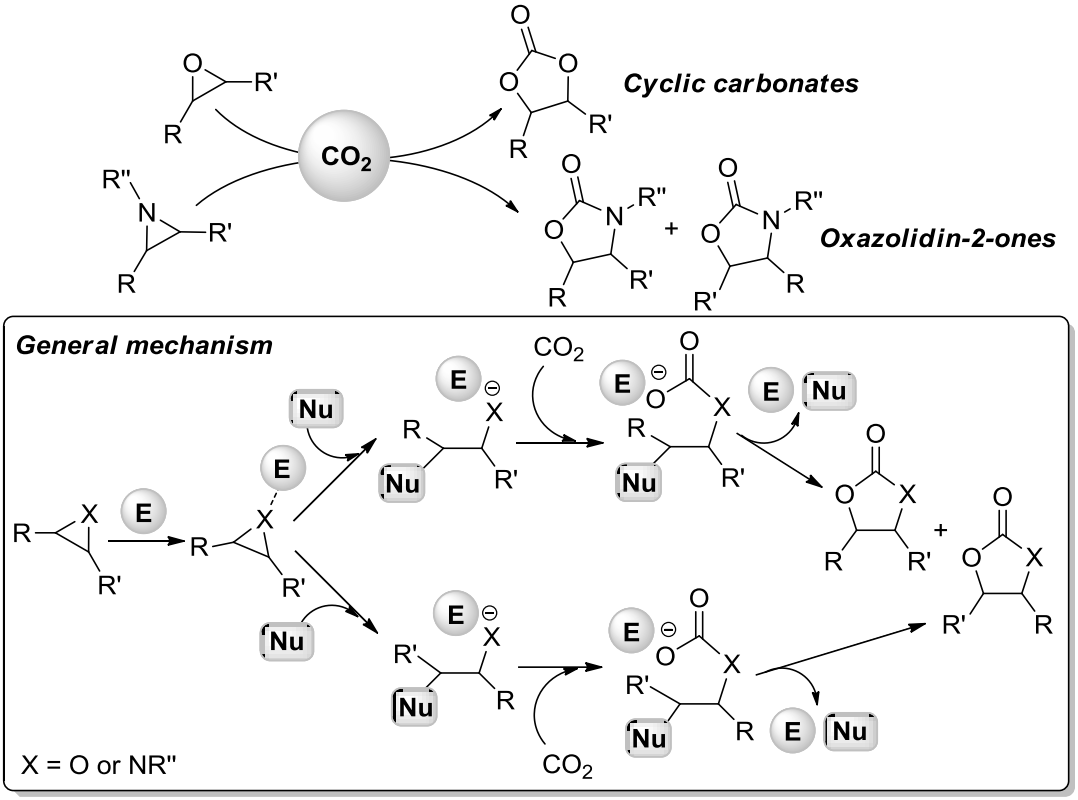


**Scheme 1**. General mechanism of $CO_2$ cycloaddition to three membered heterocycles

Alongside the most active catalysts in promoting these classes of organic transformations, porphyrin-based catalysts [22] are very efficient when used in combination with a nucleophilic source and in the last years our research group has investigated the use of porphyrin-based catalytic systems for the direct insertion of $CO_2$ in both epoxides and aziridines.

Herein we report a short account of our recent personal research, which has been focused on the use of ruthenium porphyrin complexes [23, 24] and metal-free porphyrins [25, 26], in combination with TBACl (tetrabutyl ammonium chloride), to promote the synthesis of cyclic carbonates as well as *N*-alkyl and *N*-aryl oxazolidin-2-ones.

## 2. Porphyrin-based binary systems

### *2.1. Ruthenium bis-imido complex: Ru(TPP)(NAr)$_2$/TBACl system*

Analyzing the characteristics of the previously reported catalytic mechanisms, the *'electrophilic'* nature of the involved metal seems to be necessary to coordinate and activate the three-membered ring towards the nucleophilic attack of the co-catalyst. Considering good results which were achieved in the $CO_2$ cycloaddition to epoxides promoted by porphyrin-based complexes of both main group and transition metals [13], we decided to extend the study to less *'electrophilic'* metal

promoters such as the ruthenium(VI) *bis-imido* porphyrin complex **Ru(TPP)(NAr)$_2$** [27] (TPP = dianion of *meso*-tetrakis-(phenyl) porphyrin; Ar = 3,5-$(CF_3)_2C_6H_3$) reported in table 1.

Despite of the low electrophilic character and the saturated coordinative sphere of the ruthenium (VI) atom, the binary **Ru(TPP)(NAr)$_2$**/TBACl system [24] revealed a very good activity in the synthesis of cyclic carbonate **1** (table 1), indicating that the $CO_2$ cycloaddition to epoxides does not always require the presence of an *'electrophilic'* metal centre for the substrate activation. The employment of 1% mol of **Ru(TPP)(NAr)$_2$** and 10% mol of TBACl allowed the quantitative synthesis of **1** (99% yield) under mild reaction conditions (100 °C and 0.6 MPa of $CO_2$). The very good chemical stability of the binary system permitted to be recycled for three consecutive catalytic cycles, without observing a substantial decrease of the catalytic performance. In view of these positive results, the **Ru(TPP)(NAr)$_2$**/TBACl combination was employed for the $CO_2$ cycloaddition to different epoxides affording the desired cyclic carbonates **1**-**8** in yields up to 99% (table 1). A very good activity was observed in the formation of cyclic carbonates displaying a low steric hindrance on the ring; on the other hand, more sterically encumbered substrates (or epoxides containing *tetra*-substituted carbon atoms) were less efficiently converted in the presence of the ruthenium-based catalyst.

**Table 1**. Synthesis of cyclic carbonates **1-8** promoted by **Ru(TPP)(NAr)$_2$**/TBACl[a].

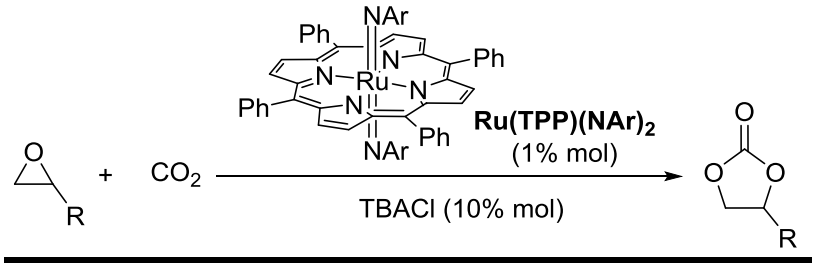


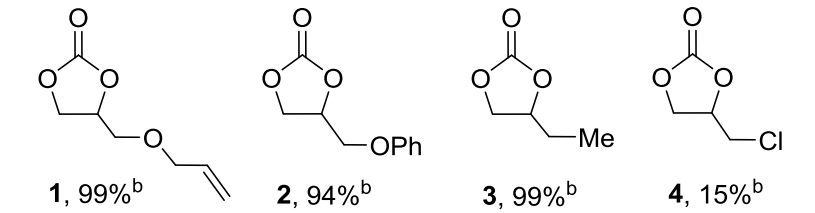


**1**, 99%[b] **2**, 94%[b] **3**, 99%[b] **4**, 15%[b]

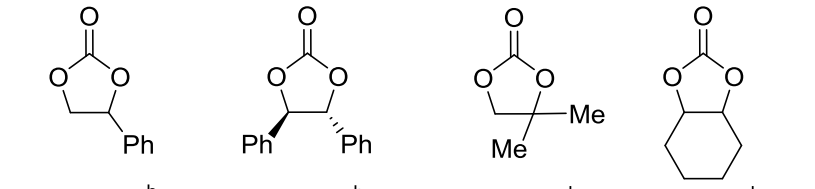


**5**, 99%[b] **6**, 65%[b] **7**, 15%[b] **8**, 17%[b]

[a]Reaction conditions: **Ru(TPP)(NAr)$_2$**/TBACl/epoxide = 1:10:100 in benzene. Reactions were performed in a steel autoclave for 8.0 h at 100 °C and 0.6 MPa of $CO_2$. [b]Determined by $^1$H-NMR spectroscopy by using 2,4-dinitrotoluene as the internal standard (uncertainty calculation: ±1%).

In view of data described above, we also investigated the **Ru(TPP)(NAr)$_2$**/TBACl activity in the less studied $CO_2$ cycloaddition to *N*-alkyl aziridines [23]. Bearing in mind that the $CO_2$ insertion into an aziridine molecule produces two different regioisomers (**A** = 5-substituted oxazolidin-2-one and **B** = 4-substituted oxazolidin-2-one) depending on the carbon atom involved in the ring opening reaction (scheme 1), the efficiency of the employed catalytic system must be estimated considering both the yield and **A**/**B** regioselectivity of the oxazolidin-2-one synthesis. The model reaction between $CO_2$ and *N*-butyl phenyl aziridine, catalyzed by **Ru(TPP)(NAr)$_2$**/TBACl, afforded the corresponding oxazolidinone in 71% yield and **9A**/**9B** ratio of 90:10 (table 2) suggesting that the proposed methodology can be employed for an efficient and regioselective synthesis of *N*-alkyl oxazolidin-2-ones. The good compromise between yield and **A**/**B** selectivity was reached under 0.6 MPa of $CO_2$ and 100 °C and consequently, these experimental conditions were employed to study the reaction scope by testing differently substituted *N*-alkyl aziridines. Desired *N*-alkyl oxazolidin-2-ones were obtained with moderate to good yields and **A**/**B** ratio up to 99:1 (table 2); collected data revealed that the reaction productivity was strongly influenced by steric factors, as already observed in the case of the cyclic carbonate synthesis. However, unlike the epoxide molecule, the aziridine ring presents an additional R group on the nitrogen atom which can

influence the efficiency of the $CO_2$ cycloaddition reaction. In fact, obtained catalytic data showed that reaction yields decreased by increasing the steric hindrance on the aziridine nitrogen atom (compare yields of products **10** and **11**, table 2). On the other hand, the steric hindrance on the carbon atom of the aziridine ring did not have an impact on catalytic performances (see products **21**-**23**, table 2). It is important to note that, in spite of the low yields observed when substrates containing very hindered nitrogen atoms were tested (see products **11** and **16**, table 2), the **Ru(TPP)(NAr)$_2$**/TBACl system maintained its high regioselectivity affording the regioisomer **A** as either the major or sole reaction product. Moreover, the robustness of the **Ru(TPP)(NAr)$_2$**/TBACl combination allowed performing three consecutive catalytic reactions affording product **9** in 70% of global yield and **A**/**B** ratio of 90:10.

**Table 2**. Synthesis of *N*-alkyl oxazolidin-2-ones **9**-**23** promoted by **Ru(TPP)(NAr)$_2$**/TBACl catalytic system[a].

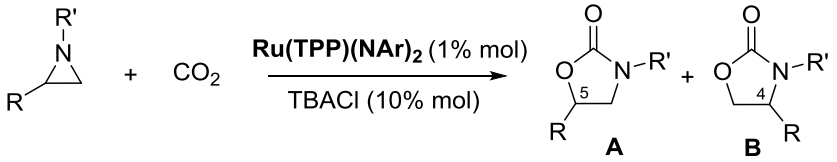


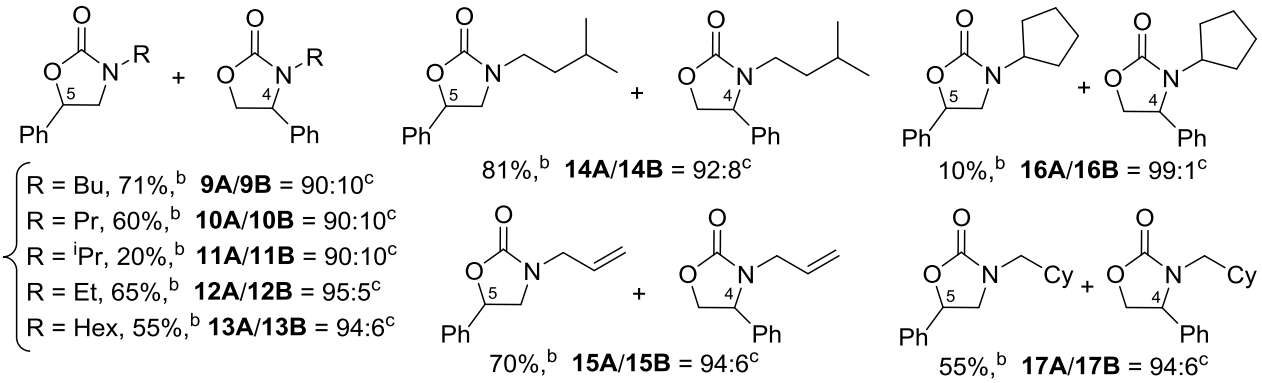


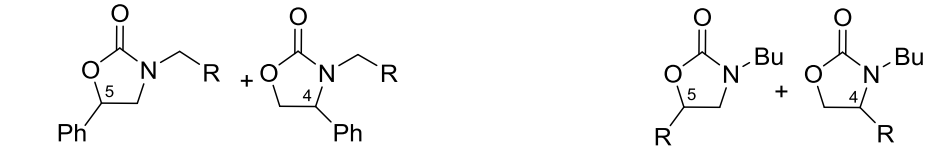


[a]Reaction conditions: **Ru(TPP)(NAr)$_2$**/TBACl/aziridine = 1:10:100 in benzene. Reactions were performed in a steel autoclave for 6.0 h at 100 °C and 0.6 MPa of $CO_2$. [b]Isolated yields. [c]Determined by $^1$H-NMR spectroscopy by using 2,4-dinitrotoluene as the internal standard (uncertainty calculation: ±1%).

To shade some light on the role of **Ru(TPP)(NAr)$_2$** in the catalytic $CO_2$ cycloaddition to three-membered rings, the $CO_2$ cycloaddition to both epoxides and aziridines were analyzed by

ESI-MS, $^1$H-NMR and IR(ATR) spectroscopies at the end of catalytic reactions. Achieved data revealed in both cases the presence of a new ruthenium species that was identified as the catalytically inactive complex **24** (scheme 2). The formation of the latter compound, probably due to a dead-end reaction that occurred independently from the presence of the three-membered ring, suggested an interaction between $CO_2$ and the *imido* axial ligand on the ruthenium atom, as proposed by the reaction mechanism reported in scheme 2. Even if the suggested mechanism was not fully verified by experimental data, the isolation of complex **24** strongly supported the key role of the ruthenium *imido* nitrogen atom, which can interact with carbon dioxide thanks to its high electron density [28-30].

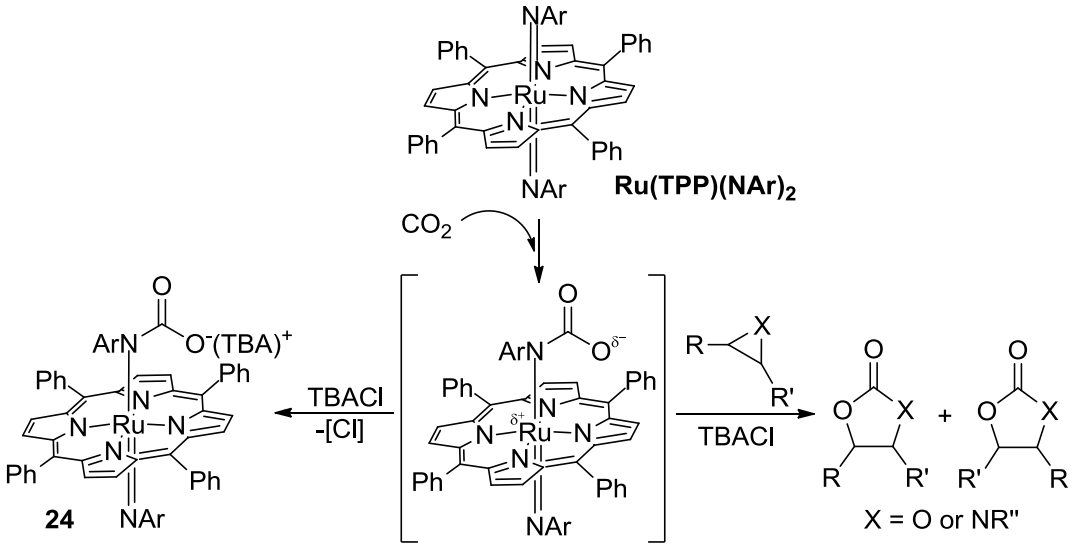


**Scheme 2**. Formation of complex **24** and proposed mechanism for the $CO_2$ cycloaddition to three-membered rings promoted by **Ru(TPP)(NAr)$_2$**/TBACl binary system.

### *2.2. Metal-free porphyrin: TPPH$_2$/TBACl system*

The interaction between carbon dioxide and ruthenium *imido* nitrogen atoms, supported by the observation of complex **24**, prompted us to research alternative nitrogen atoms capable to activate the $CO_2$ cycloaddition towards three-membered ring compounds. Considering the ever-increasing demand of inexpensive, non-toxic, and easily to handle catalysts, we tested the activity of metal-free porphyrin/TBACl combinations in the synthesis of *N*-alkyl oxazolidin-2-ones [26]. Surprisingly, we discovered that the $CO_2$ cycloaddition to *N*-alkyl aziridines also occurred in the absence of a metal-based catalyst and it can be promoted by using the simple combination of metal-free porphyrins and ammonium salts. In addition, the lack of a metal species allows employing any type of reaction solvents, including coordinating ones that usually deactivate the catalyst by saturating the coordination sphere.

Comparing the activity of different metal-free porphyrins, such as **$TPPH_2$** (*meso*-tetrakis-(phenyl)porphyrin), **4-$^t$BuTPPH$_2$** (*meso*-tetrakis(4-*tert*-butylphenyl) porphyrin), **4-$CF_3$TPPH$_2$** (*meso*-tetrakis(4-trifluoromethylphenyl) porphyrin), **4-COOHTPPH$_2$** (*meso*-tetrakis(4-carboxyphenyl) porphyrin), **$F_5$TPPH$_2$** (5-(pentafluorophenyl)-10,15,20-triphenyl porphyrin), **$F_{20}$TPPH$_2$** (*meso*-tetrakis(pentafluorophenyl) porphyrin) and **OEPH$_2$** (octaethylporphyrin), we observed a limited influence of the electronic and steric features of the employed porphyrin on catalytic performances.

In view of the non-toxicity, commercial availability and the easily synthetic procedure to obtain the unsubstituted **$TPPH_2$**, we employed the low-cost **$TPPH_2$**/TBACl binary system to catalyse the synthesis of several *N*-alkyl oxazolidin-2-ones. Several compounds were efficiently obtained in yields up to 100% and **A/B** ratios up to 99:1 (table 3) under the optimized experimental conditions of 125 °C, 1.2 MPa of $CO_2$ and **$TPPH_2$**/TBACl/aziridine ratio of 1:5:100. The study of the reaction scope revealed again that the steric hindrance on the aziridine nitrogen atom is one of the most important parameters that influences the catalytic efficiency, as observed by comparing the yields of products **9A/9B** and **26A/26B** in which the *n*-butyl group on the aziridine nitrogen atom was replaced by the more hindered *tert*-butyl one. The same tendency was observed in the case of the synthesis of products **16A/16B** and **27A/27B** in which the enlargement of the ring placed on the *N*-aziridine atom produced a clear decrease of the reaction yield (from 95% yield for **16A/16B** to 52% yield for **27A/27B**). However, in all cases the steric hindrance of the aziridine molecule did not affect the **A/B** regioselectivity and the regioisomer **A** was always obtained as the major product (**A/B** ratios up to 99:1).

**Table 3**. Synthesis of *N*-alkyl oxazolidin-2-ones promoted by **TPPH$_2$**/TBACl system[a].

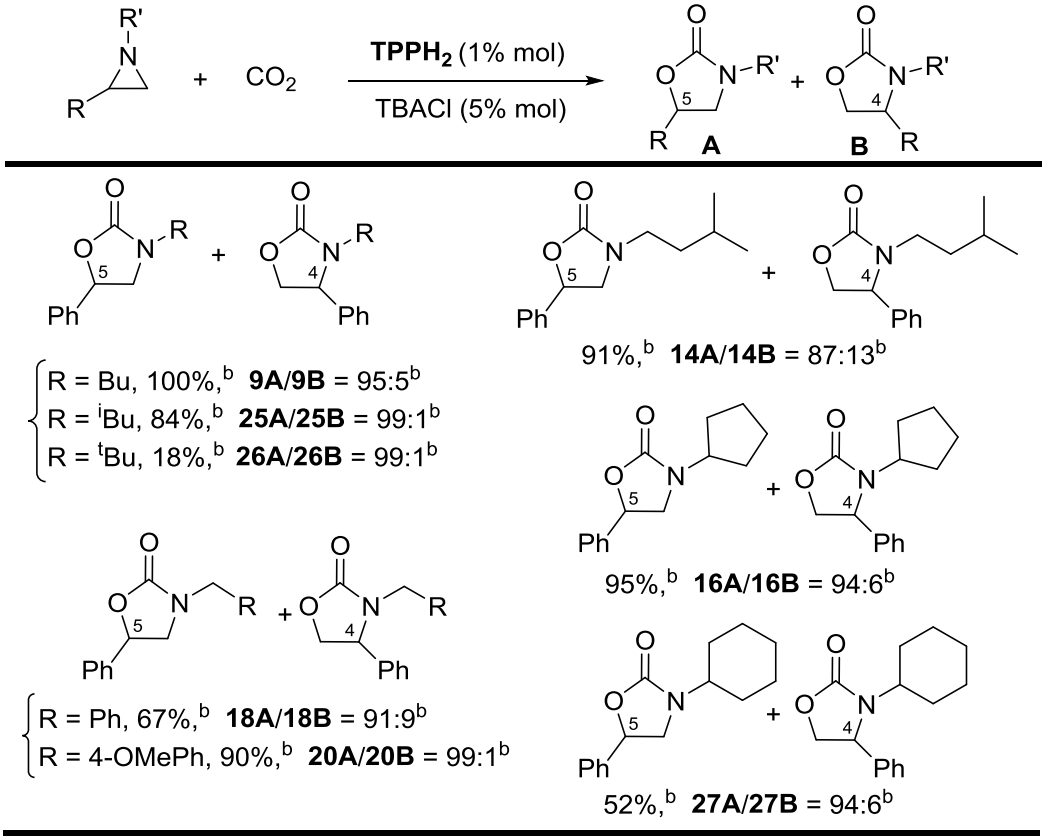


[a]Reaction conditions: **TPPH$_2$**/TBACl/aziridine = 1:5:100 in THF. Reactions were performed in a steel autoclave for 6.0 h at 125 °C and 1.2 MPa of $CO_2$. [b]Determined by $^1$H-NMR spectroscopy by using 2,4-dinitrotoluene as the internal standard (uncertainty calculation: ±1%).

The comparison of catalytic performances of **Ru(TPP)(NAr)$_2$** and **TPPH$_2$** in the $CO_2$ insertion into *N*-alkyl aziridines revealed that the cost-effective **TPPH$_2$**/TBACl binary system resulted more active than the metal-containing one, both in terms of yields and regioselectivities. In addition, the use of **TPPH$_2$** improved the process eco-compatibility avoiding the use of metals and allowing the replacement of the non-coordinative and unsafe benzene, necessary in presence of **Ru(TPP)(NAr)$_2$**, with the less toxic THF (tetrahydrofuran), which also favours the $CO_2$ solubilisation.

The good results reached in the $CO_2$ cycloaddition to *N*-alkyl aziridines inspired us to test the **TPPH$_2$**/TBACl binary system in the more challenging synthesis of *N*-aryl oxazolidin-2-ones [25], whose moiety is incorporated in some anti-microbial and anti-bacterial FDA-approved drugs such as toloxatone [31], tedizolid [32] and linezolid [33]. The lower basicity and nucleophilicity of *N*-aryl aziridines, with respect to the *N*-alkyl ones, implies a limited reactivity towards carbon dioxide and consequently it explains the lack of general methodologies for the synthesis of *N*-aryl oxazolidin-2-ones by the direct insertion of $CO_2$ into *N*-aryl aziridines. Despite this drawback, the **TPPH$_2$**/TBACl binary system was capable to catalyse the ambitious $CO_2$ cycloaddition to *N*-aryl

aziridines providing 18 examples of differently substituted *N*-aryl oxazolidin-2-ones (products **28-45**, table 4).

*N*-aryl oxazolidin-2-ones were obtained in yields up to 99% and **A**/**B** regioselectivities up to 99:1 by employing the following optimized reaction conditions: **TPPH$_2$**/TBACl/aziridine = 1:5:100; *N*-aryl aziridine concentration: 1.5 M; solvent: THF; temperature: 125 °C; $CO_2$ pressure: 1.2 MPa and time: 8 hours.

**Table 4**. Synthesis of *N*-aryl oxazolidin-2-ones **28-45** promoted by **TPPH$_2$**/TBACl system[a].

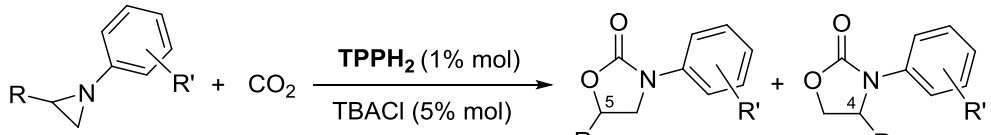


R = 3,5-$(CF_3)_2$, 99%,[b] **28A**/**28B** = 86:14[c]
R = 4-$NO_2$, 99%,[b] **29A**/**29B** = 78:22[c]
R = 4-OMe, 20%,[b] **30A**/**30B** = 99:1[c]
R = 4-$^t$Bu, 55%,[b] **31A**/**31B** = 96:4[c]
R = 4-Br, 50%,[b] **32A**/**32B** = 90:10[c]
R = 4-Cl, 72%,[b] **33A**/**33B** = 89:1[c]
R = 2-$NO_2$, 60%,[b] **34A**/**34B** = 64:36[c]
R = 3-OMe, <7%,[b] **35A**/**35B** = none
R = 3,5-$Cl_2$, 94%,[b] **36A**/**36B** = 81:19[c]
R = 3,5-$(NO_2)_2$, 30%,[b] **37A**/**37B** = 77:23[c]

R = 4-tolyl, 90%,[b] **38A**/**38B** = 80:20[c]
R = 4-$^t$BuPh, 85%,[b] **39A**/**39B** = 99:1[c]
R = 4-BrPh, 99%,[b] **40A**/**40B** = 80:20[c]
R = $C_6F_5$, 64%,[b] **41A**/**41B** = 82:18[c]

R = 4-MePh, R' = 4-$NO_2$Ph, 90%,[b] **42A**/**42B** = 85:15[c]
R = $C_6F_5$, R' = 4-$^t$BuPh, 79%,[b] **43A**/**43B** = 91:9[c]

R = 3,5-$(CF_3)_2$, 52%,[b] **44A**/**44B** = 94:6[c]
R = 4-$^t$Bu, 28%,[b] **45A**/**45B** = 83:17[c]

[a]Reaction conditions: **TPPH$_2$**/TBACl/aziridine = 1:5:100 in THF. Reactions were performed in a steel autoclave for 8.0 h at 125 °C and 0.6 MPa of $CO_2$. [b]Isolated yields. [c]Determined by $^1$H-NMR spectroscopy by using 2,4-dinitrotoluene as the internal standard (uncertainty calculation: ±1%).

The study of the reaction scope evidenced that the catalytic process can be affected by both electronic and steric features of the starting *N*-aryl aziridine, unlike the case of *N*-alkyl aziridines in which the steric hindrance on the nitrogen atom represented the most dominant parameter. From a general point of view, the presence of electron withdrawing groups (EWGs) on the *N*-aryl aziridine ring had a positive effect on the reaction productivity. However, bearing in mind the possibility to

differently functionalize the nitrogen and carbon atoms of the aziridine, the reaction yield can be improved by the co-presence of EWGs and EDGs (electron donating groups) that, with their opposite electronic properties, can induce the polarization of the aziridine C-N bond favouring the ring-opening reaction and the subsequent $CO_2$ insertion (compare the yields of products **41** and **43**). From a steric point of view, the presence of substituents on both carbon atoms of the aziridine ring caused the decrease of the reaction yield, especially in presence of EDGs on the *N*-aryl group, according to the above-described electronic effects (compare products **44A/44B** and **45A/45B**).

Considering our knowledge in the synthesis of *N*-aryl aziridines by **Ru(TPP)CO**-catalyzed procedures [34-37], we finally applied a tandem methodology to further improve the eco-sustainability of the *N*-aryl oxazolidin-2-ones' synthesis.

As reported in scheme 3, we synthesized the *N*-aryl oxazolidin-2-ones **28** and **30** by a two-step process in which the intermediate *N*-aryl aziridine was first synthesized and directly used for the subsequent reaction with carbon dioxide without being isolated from the reaction mixture. It is important to note that products **28** and **30** were obtained in yields and regioselectivities comparable to those achieved by using the standard process in which the starting aziridine was first synthesized, isolated, purified and then reacted with $CO_2$ (compare data reported in table 4 and scheme 3). The developed tandem procedure enhanced the eco-compatibility of the process cycloaddition by combining the use of $CO_2$ with the formation of molecular nitrogen as the sole benign by-product of the *N*-aryl aziridines synthesis. Moreover, the cost-effectiveness of the reaction was enhanced by avoiding expensive and long purification steps of the *N*-aryl aziridine isolation. In addition, the tandem procedure allowed to selectively synthesise the regioisomer **A** of the pharmaceutically active *N*-aryl oxazolidin-2-one **46** in 35% yield, which is a better yield than that previously reported for the synthesis of **46** by an epoxide-based procedure [38].

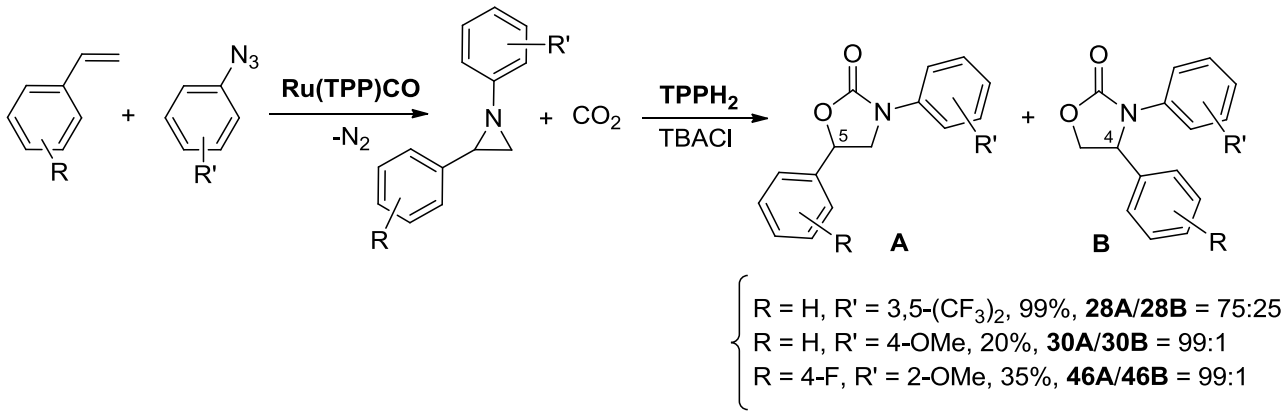


**Scheme 3**. Tandem synthesis of *N*-aryl oxazolidin-2-ones **28, 30** and **46**.

In view of all the positive results obtained in the synthesis of both *N*-alkyl and *N*-aryl oxazolidin-2-ones catalyzed by the convenient **$TPPH_2$**/TBACl binary system, the reaction mechanism was explored by DFT calculations (obtained results are illustrated in detail in the following section). Computational data revealed the key role of the **$TPPH_2$**/TBACl adduct **C** (scheme 4) that represents the real active catalyst in the $CO_2$ cycloaddition to aziridines. As reported in the proposed general reaction mechanism (scheme 4) the adduct **C** activates the aziridine ring towards the nucleophilic attack of the halogen atom (intermediates **D**-**E**) allowing the subsequent $CO_2$ coupling (intermediate **F**) and the final formation of the regioisomer **A**, as the major oxazolidin-2-one.

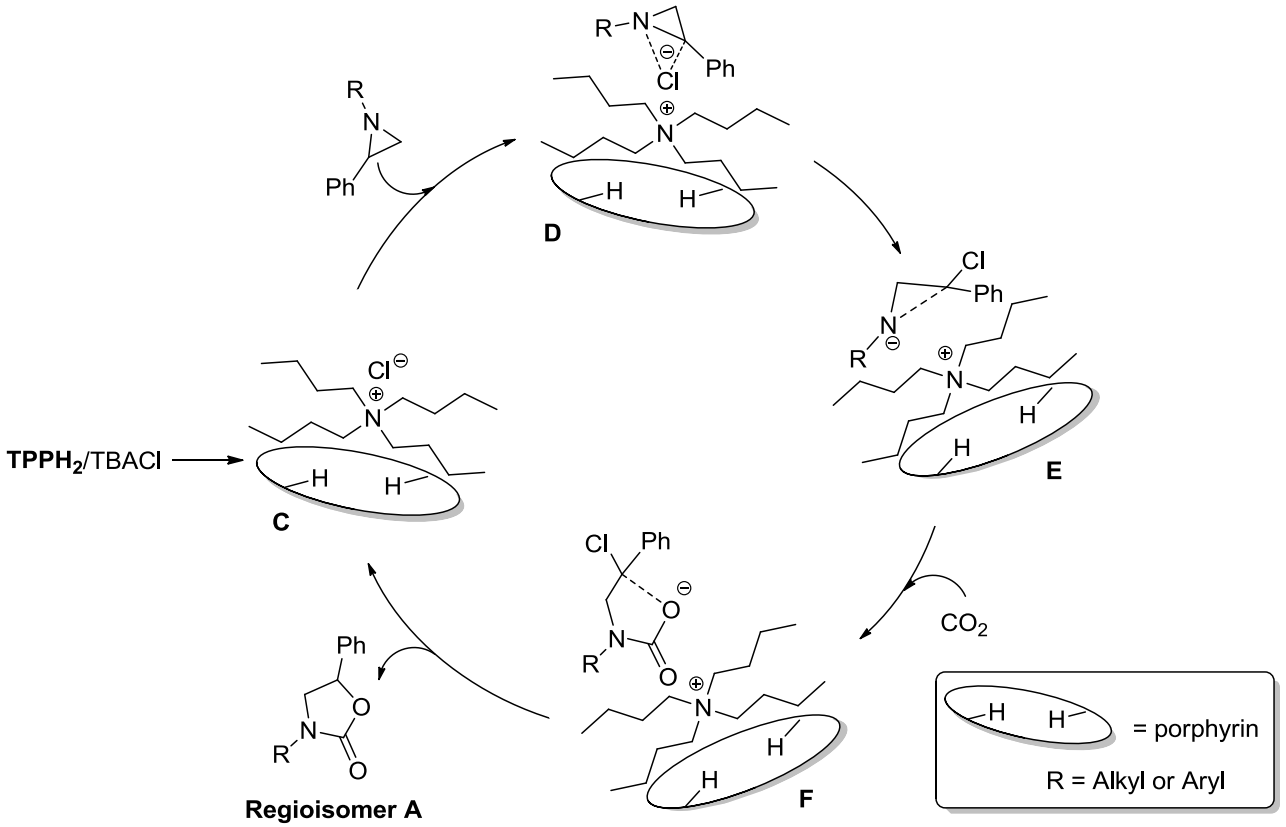


**Scheme 4**. Proposed mechanism for the $CO_2$ cycloaddition to *N*-alkyl and *N*-aryl aziridines catalyzed by the **$TPPH_2$**/TBACl system

## 3. DFT Calculations

As reported above, experimental data indicated that **Ru(TPP)(NAr)$_2$** and **$TPPH_2$** were both able in promoting cycloaddition reactions when used in combination with TBACl. However, considering the better eco-sustainability of metal-free catalyzed processes, only the mechanism of the reaction

promoted by **TPPH$_2$**/TBACl binary system was investigated in details from a theoretical point of view at B97D-DFT level of theory [39]. A deep understanding of the homogeneous catalytic processes has been obtained by identifying both intermediates and Transition States, which are hardly to be experimentally detected but are fundamental to predict mechanistic routes. The DFT study of the $CO_2$ cycloaddition to *N*-alkyl aziridine promoted by **TPPH$_2$**/TBACl system was performed by using *N*-butyl aziridine as the model substrate (all the encountered intermediates and the Transition States are indicated with the apex $^{Bu}$). The formation of different potential adducts between **TPPH$_2$** and, alternatively, one of the other three reaction components (TBACl, $CO_2$, aziridine) has been investigated and the most probable first step of the reaction should be the formation of the adduct **C** of scheme 4, between TBACl and **TPPH$_2$**, with a free energy gain of -7.5 kcal mol$^{-1}$ (figure 1). The peripheral *meso* phenyl substituents of the porphyrin macrocycle forms a cradle where the butyl moieties of the $TBA^+$ cation are lying down through weak cooperative dispersion forces and C-H/$\pi$ interactions between the positively charged $TBA^+$ cation and aromatic moieties [40].

The formation of the adduct between **TPPH$_2$** and TBACl may weaken the ion pair strength of the salt to render the chloride ion more prone to attack aziridine and cause the ring opening reaction [25]. The other two adducts, namely **TPPH$_2$**/$CO_2$ and **TPPH$_2$**/aziridine, have been discarded for energetic reasons and for a hindered further evolution of the reactivity, respectively.

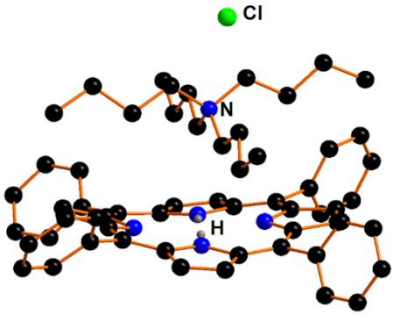


**Figure 1.** Optimized structure of the adduct **C** between **TPPH$_2$** and TBACl salt. The hydrogen atoms are omitted for clarity.

Then, the adduct **C** is ready to interact with aziridine, through the formation of the intermediate **D$^{Bu}$** of scheme 4 [26], featuring a shorter distance between the chloride ion and the most substituted $C_1$ carbon of the aziridine, with respect to $C_2$ atom, clarifying the selectivity in the ring opening site (figure 2). The chloride ion is able to perform the nucleophilic attack at the $C_1$ atom through the formation of Transition State (**TS$_1^{Bu}$**) with a free energy barrier of *ca*. +35 kcal mol$^{-1}$ (figure 2). The

particularly high free energy cost required for by-passing the $\mathbf{TS_1^{Bu}}$ is in line with the high experimental temperature that is necessary for this reaction.

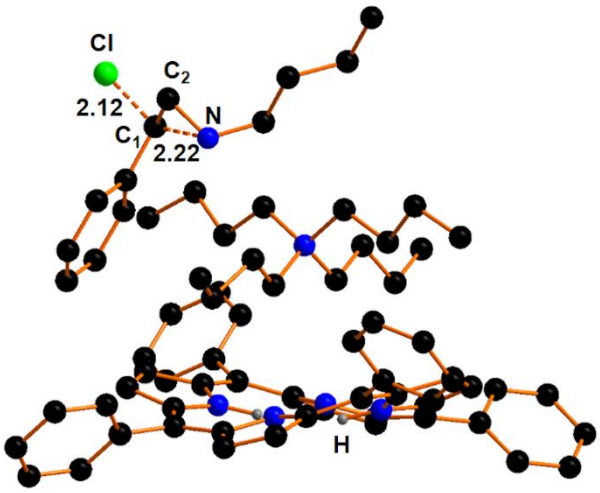


**Figure 2.** Transition State, $\mathbf{TS_1^{Bu}}$, for the aziridine opening by the chloride. The hydrogen atoms are omitted for clarity.

The N─$C_1$ distance appears particularly elongated in $TS_1$ and the negative charge, initially on the chlorine, is transferred to the nitrogen centre of the open intermediate $\mathbf{E^{Bu}}$ (figure 3), which acquires an amidic character, able to activate electrophilic species, such as $CO_2$. The high energy cost required for the $TS_1$ is partially compensated (-22.5 kcal $mol^{-1}$) by the formation of the bond between the amidic nitrogen and the carbon atom of $CO_2$, which is associated with a N→O electron transfer in the formation of $\mathbf{F^{Bu}}$ intermediate (figure 3).

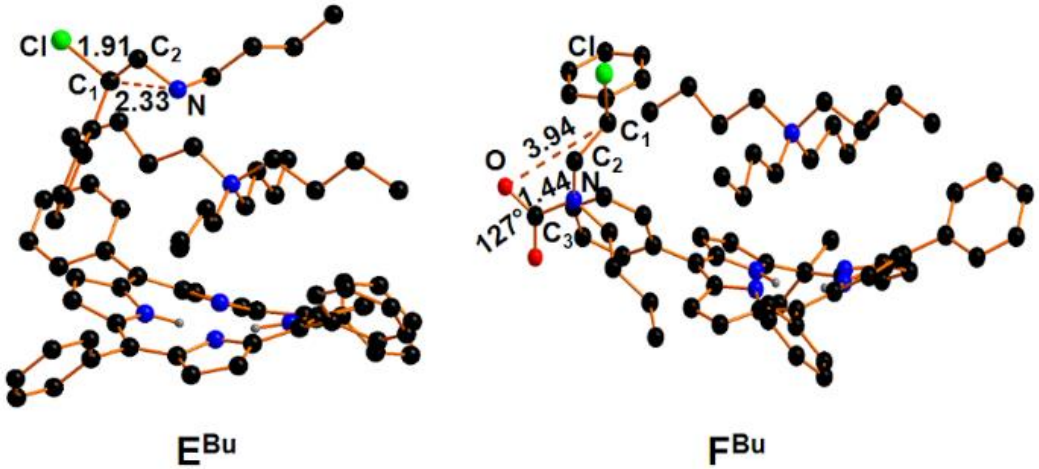


**Figure 3.** Optimized structure of $\mathbf{E^{Bu}}$ and $\mathbf{F^{Bu}}$ intermediates. The hydrogen atoms are omitted for clarity.

This causes the formation of a bent $CO_2$ structure with the appearance of active IR modes around 1700 $cm^{-1}$ that are associated with the C=O stretching. The charge transfer from the nitrogen to the $CO_2$ group allows a localization of electron density at the oxygen centres with the enhancement of their nucleophilic abilities, which are able to attack the $C_1$ atom to promote the ring closure to oxazolidin-2-one, with a free energy gain larger than 31 kcal $mol^{-1}$. The required free energy barrier for reaching the $\mathbf{TS_2^{Bu}}$, shown in figure 4, is only 9.4 kcal $mol^{-1}$.

In the $\mathbf{TS_2^{Bu}}$, the $C_1$ centre features a trigonal bi-pyramidal coordination (one hydrogen is omitted for clarity) with the formation of a $C_1$─O bond ($C_1$─O distance 2.43 Å) and the cleavage of the $C_1$─Cl one (Cl─$C_1$ is 2.22 Å).

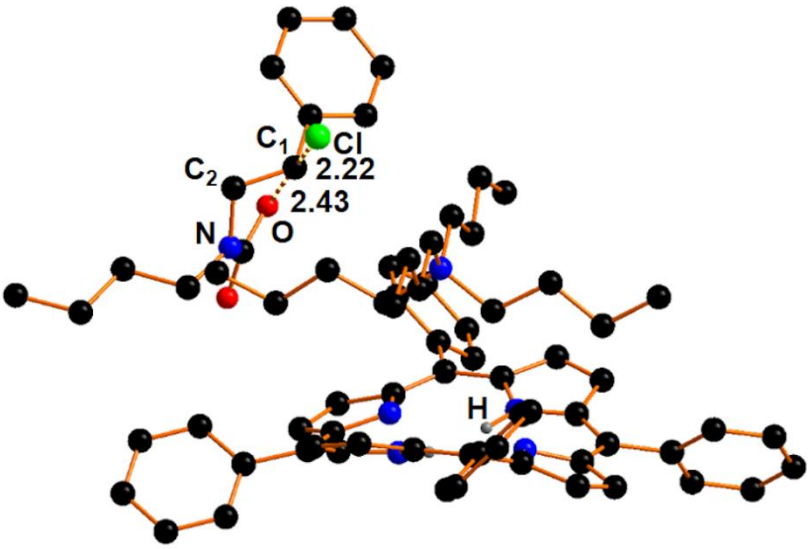


**Figure 4.** Transition State $\mathbf{TS_2^{Bu}}$ for the formation of oxazolidin-2-one. The hydrogen atoms are omitted for clarity.

The computational analysis perfectly agrees with mechanism proposed in scheme 4 with an overall free energy gain of -4.7 kcal $mol^{-1}$ for the insertion reaction of the $CO_2$ into the aziridine skeleton to provide the *N*-butyl oxazolidin-2-one regioisomer $\mathbf{A^{Bu}}$. In addition, DFT calculations have highlighted the real nature of the catalyst, namely the binary $\mathbf{TPPH_2}$/TBACl adduct.

A detailed free energy pathway for the catalytic $CO_2$ insertion reaction into the *N*-butyl aziridine ring has been reported in black in scheme 5. The geometric structure of the main intermediates and Transition States are highlighted in scheme 5 while the main structural features are reported in table 5.

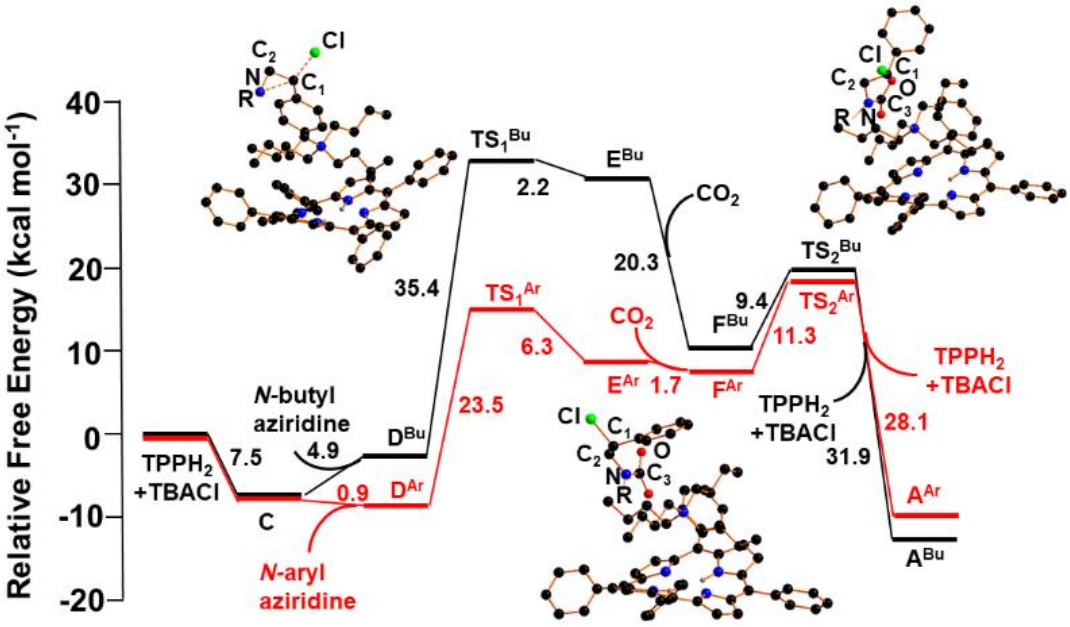


**Scheme 5.** Free energy profile (kcal $mol^{-1}$) for the formation of a) *N*-butyl oxazolidin-2-one (in black) and b) *N*-aryl oxazolidin-2-one (in red).

**Table 5.** Main structural features (distances and angles) of the most important intermediates or Transition States with butyl or aryl substituents.

| **Compound** | N-$C_1$ (Å) | $C_1$-Cl (Å) | N-$C_3$ (Å) | O-$C_1$ (Å) | O-$C_3$-O (°) | O-$C_1$-Cl (°) |
|---|---|---|---|---|---|---|
| $\mathbf{TS_1^{Bu}}$ | 2.22 | 2.12 | - | - | - | - |
| $\mathbf{TS_1^{Ar}}$ | 2.23 | 2.44 | - | - | - | - |
| $\mathbf{E^{Bu}}$ | 2.33 | 1.91 | - | - | - | - |
| $\mathbf{E^{Ar}}$ | 1.94 | 2.48 | - | - | - | - |
| $\mathbf{F^{Bu}}$ | 2.36 | 1.91 | 1.44 | 3.94 | 127.0 | 117.1 |
| $\mathbf{F^{Ar}}$ | 2.38 | 1.89 | 1.52 | 3.83 | 129.6 | 120.6 |
| $\mathbf{TS_2^{Bu}}$ | 2.35 | 2.22 | 1.43 | 2.43 | 127.7 | 176.9 |
| $\mathbf{TS_2^{Ar}}$ | 2.36 | 2.32 | 1.48 | 2.14 | 128.0 | 173.2 |

The replacement of the butyl substituent with an aryl group at the aziridine nitrogen atom causes some substantial energetic variations, as shown in the red pathway of scheme 5, with the intermediates and/or Transition States indicated with the apex $^{Ar}$. Similarly to what described for the reaction of *N*-butyl aziridine, the first step is the formation of the adduct **C** between the $\mathbf{TPPH_2}$ and the TBACl salt followed by the interaction of this active adduct with *N*-aryl aziridine. In contrast

with the butyl case, the formation of the adduct $\mathbf{D^{Ar}}$ is slightly exergonic (-0.9 kcal $mol^{-1}$) compared to the endergonic one that was modelled for the butyl case $\mathbf{D^{Bu}}$ (+4.9 kcal $mol^{-1}$) [25].

The free energy barrier associated with the achievement of the Transition State $\mathbf{TS_1^{Ar}}$ is significantly lower than that encountered for the $\mathbf{TS_1^{Bu}}$ (23.5 *vs*. 35.4 kcal $mol^{-1}$). This difference is responsible for an easier nucleophilic attack of the chloride ion to *N*-aryl aziridine rather than *N*-butyl one, as also confirmed from the structural comparison of data reported in table 5. In this regards, even if the chloride anion in $\mathbf{TS_1^{Ar}}$ is at the long distance of 2.44 Å from $C_1$, it is able to elongate the N─$C_1$ distance to 2.23 Å. On the other hand, in $\mathbf{TS_1^{Bu}}$ the chloride ion can enforce its nucleophilic power only at the smaller distance of 2.12 Å. This difference suggests a somewhat hindered process for the *N*-butyl derivative with respect the process involving the *N*-aryl one. The situation is reverse after the cleavage of the N-$C_1$ bond and the formation of the $C_1$-Cl one. In fact, the nitrogen centre of $\mathbf{E^{Ar}}$ seems less nucleophilic toward $CO_2$, as confirmed by a free energy gain of only -1.7 kcal $mol^{-1}$ for the formation of $\mathbf{F^{Ar}}$, compared to the same process modelled for the formation of $\mathbf{F^{Bu}}$ (-20.3 kcal $mol^{-1}$). The most efficient formation of intermediate $\mathbf{F^{Bu}}$ provides also a more efficient N→$C_3$ electron transfer, thus more electron density at the $CO_2$ unit and a red shift (100 $cm^{-1}$ *ca*.) for the IR active CO stretching (1674 *vs*. 1575 $cm^{-1}$for $\mathbf{F^{Ar}}$ and $\mathbf{F^{Bu}}$, respectively). This process was also responsible for a less nucleophile character of the oxygen centre in $\mathbf{F^{Ar}}$, as also confirmed for a slightly higher free energy barrier (2 kcal $mol^{-1}$ *ca*.) for the achievement of $\mathbf{TS_2^{Ar}}$, compared to that of $\mathbf{TS_2^{Ar}}$. The final ring closure allows the restoration of the catalyst $\mathbf{TPPH_2}$/TBACl adduct with a total free energy gain for the aryl case halved with respect to that of the butyl one (-2.2 *vs*. -4.7 kcal $mol^{-1}$).

Thus, although the first energy barrier is lower for the aryl case, the second part is more feasible for the alkyl one with the net result that *N*-butyl aziridines are always more reactive towards $CO_2$ than *N*-aryl ones. It should be noted that in both cases the reactions involve high free energy barriers that can be bypassed thanks to the applied high experimental temperatures.

Once investigated in details the different steps of the insertion reaction, a screening has been carried out in order to establish potential correlations between the nature of the porphyrin structure and the catalytic activity of the system. Obtained results underlined that the energetic profile of the reaction is almost independent from the electronic nature of substituents at the *meso* aryl rings of the porphyrin (*e.g.* $\mathbf{4\text{-}COOHTPPH_2}$ and $\mathbf{F_{20}TPPH_2}$) and in all cases the formation of the initial porphyrin/TBACl adduct is strongly favoured.

## 4. Conclusions and future perspectives

The present short account provides an overview of our recent results achieved on the employment of porphyrin-based catalysts for the direct insertion of $CO_2$ into three-membered rings, such as epoxides and aziridines. Obtained results displayed the possibility to employ ruthenium(VI) *bis-imido* porphyrin complexes for the efficient synthesis of cyclic carbonates and *N*-alkyl oxazolidin-2-ones. However, deeply investigations allowed to replace the ruthenium complex **Ru(TPP)(NAr)$_2$** with **TPPH$_2$**, a low-cost metal-free porphyrin which showed better performances than the ruthenium counterpart in the synthesis of *N*-alkyl oxazolidin-2-ones. Unexpectedly, the cost-effective combination of **TPPH$_2$** and TBACl efficiently catalyzed the more challenging synthesis of *N*-aryl oxazolidin-2-ones and allowed providing a tandem methodology, which did not require the aziridine purification, useful to also promote the synthesis of a pharmaceutically active *N*-aryl oxazolidin-2-one. The symbiotic experimental/computational approach allowed suggesting a reaction mechanism in which the adduct formed by **TPPH$_2$** and TBACl represented the catalytically active species. The **TPPH$_2$**/TBACl adduct played the pivotal role by activating the aziridine ring towards the nucleophilic attack of the halogen atom and by reducing the free energy barrier which is normally required for the uncatalyzed $CO_2$ cycloaddition to *N*-alkyl and *N*-aryl aziridines.

The present account highlights how the combination of experimental and computational studies could be a valuable tool to fine-tune the properties of catalytic systems suitable to develop sustainable protocols for the conversion of waste materials, such as $CO_2$, in high added value compounds. The great versatility of porphyrin ligands as platforms for the activation of different substrates and for the promotion of $CO_2$ insertion reactions may be used to develop smart materials capable of combining the capture and valorisation of carbon dioxide. In addition, in view of the role played by the porphyrin ring, whose nitrogen atoms are directly involved in the formation of the catalytic active species, the described studies open the way to the development of new sustainable methodologies in which the metal-free porphyrin moiety can be employed to favour nucleophilic attacks to low reactive electrophiles.

## References

[1] H. Stančin, H. Mikulčić, X. Wang, N. Duić, Renew. Sust. Energ. Rev., 128 (2020) 109927.

[2] L.R. Amjith, B. Bavanish, Chemosphere, 293 (2022) 133579.

[3] A.D.N. Kamkeng, M. Wang, J. Hu, W. Du, F. Qian, Chem. Eng. J., 409 (2021) 128138.

[4] J. Zhang, C.D. Sewell, H. Huang, Z. Lin, Adv. Energy Mater., 11 (2021) 2102767.

[5] M.N. Anwar, A. Fayyaz, N.F. Sohail, M.F. Khokhar, M. Baqar, A. Yasar, K. Rasool, A. Nazir, M.U.F. Raja, M. Rehan, M. Aghbashlo, M. Tabatabaei, A.S. Nizami, J. Environ. Manage., 260 (2020) 110059.
[6] J. Artz, T.E. Müller, K. Thenert, J. Kleinekorte, R. Meys, A. Sternberg, A. Bardow, W. Leitner, Chem. Rev., 118 (2018) 434-504.
[7] A.J. Kamphuis, F. Picchioni, P.P. Pescarmona, Green Chem., 21 (2019) 406-448.
[8] E.J.C. Lopes, A.P.C. Ribeiro, L.M.D.R.S. Martins, Catalysts, 10 (2020) 479.
[9] A. Rehman, F. Saleem, F. Javed, A. Ikhlaq, S.W. Ahmad, A. Harvey, J. Environ. Chem. Eng., 9 (2021) 105113.
[10] S. Pulla, C.M. Felton, P. Ramidi, Y. Gartia, N. Ali, U.B. Nasini, A. Ghosh, J. CO2 Util., 2 (2013) 49-57.
[11] T. Niemi, T. Repo, Eur. J. Org. Chem., 2019 (2019) 1180-1188.
[12] R.R. Shaikh, S. Pornpraprom, V. D'Elia, ACS Catal., 8 (2018) 419-450.
[13] C. Damiano, P. Sonzini, D. Intrieri, E. Gallo, J. Porphyr. Phthalocyanines, 24 (2020) 809-816.
[14] L. Guo, K.J. Lamb, M. North, Green Chem., 23 (2021) 77-118.
[15] W.-L. Dai, S.-L. Luo, S.-F. Yin, C.-T. Au, Appl. Catal. A: Gen., 366 (2009) 2-12.
[16] C. Calabrese, F. Giacalone, C. Aprile, Catalysts, 9 (2019) 325.
[17] S.-L. Hou, J. Dong, B. Zhao, Adv. Mater., 32 (2020) 1806163.
[18] R. Luo, X. Liu, M. Chen, B. Liu, Y. Fang, ChemSusChem, 13 (2020) 3945-3966.
[19] C. Claver, M.B. Yeamin, M. Reguero, A.M. Masdeu-Bultó, Green Chem., 22 (2020) 7665-7706.
[20] F.N. Al-Rowaili, U. Zahid, S. Onaizi, M. Khaled, A. Jamal, E.M. Al-Mutairi, J. CO2 Util., 53 (2021) 101715.
[21] Y. Shi, S. Hou, X. Qiu, B. Zhao, Top. Curr. Chem., 378 (2020) 11.
[22] D. Intrieri, C. Damiano, P. Sonzini, E. Gallo, J. Porphyr. Phthalocyanines, 23 (2019) 305-328.
[23] D. Carminati, E. Gallo, C. Damiano, A. Caselli, D. Intrieri, Eur. J. Inorg. Chem., 2018 (2018) 5258-5262.
[24] C. Damiano, P. Sonzini, D. Intrieri, E. Gallo, J. Porphyr. Phthalocyanines, 24 (2020) 809-816.
[25] P. Sonzini, C. Damiano, D. Intrieri, G. Manca, E. Gallo, Adv. Synth. Catal., 362 (2020) 2961-2969.
[26] C. Damiano, P. Sonzini, G. Manca, E. Gallo, Eur. J. Org. Chem., 2021 (2021) 2807-2814.
[27] C. Damiano, P. Sonzini, A. Caselli, E. Gallo, Chapter Three - Imido complexes of groups 8–10 active in nitrene transfer reactions, in: P.J. Pérez (Ed.) Adv. Organomet. Chem., Academic Press2021, pp. 145-184.

[28] G. Manca, E. Gallo, D. Intrieri, C. Mealli, ACS Catal., 4 (2014) 823-832.
[29] D. Intrieri, D.M. Carminati, P. Zardi, C. Damiano, G. Manca, E. Gallo, C. Mealli, Chem. Eur. J., 25 (2019) 16591-16605.
[30] G. Manca, C. Mealli, D.M. Carminati, D. Intrieri, E. Gallo, Eur. J. Inorg. Chem., 2015 (2015) 4885-4893.
[31] F. Moureau, J. Wouters, D.P. Vercauteren, S. Collin, G. Evrard, F. Durant, F. Ducrey, J.J. Koenig, F.X. Jarreau, Eur. J. Med. Chem., 27 (1992) 939-948.
[32] D. McBride, T. Krekel, K. Hsueh, M.J. Durkin, Expert Opin. Drug Metab. Toxicol., 13 (2017) 331-337.
[33] A. Zahedi Bialvaei, M. Rahbar, M. Yousefi, M. Asgharzadeh, H. Samadi Kafil, J. Antimicrob. Chemother., 72 (2017) 354-364.
[34] C. Damiano, D. Intrieri, E. Gallo, Inorg. Chim. Acta, 470 (2018) 51-67.
[35] S. Rossi, A. Puglisi, D. Intrieri, E. Gallo, J. Flow Chem., 6 (2016) 234-239.
[36] S. Rossi, A. Puglisi, M. Benaglia, D.M. Carminati, D. Intrieri, E. Gallo, Catal. Sci. Technol., 6 (2016) 4700-4704.
[37] P. Zardi, A. Pozzoli, F. Ferretti, G. Manca, C. Mealli, E. Gallo, Dalton Trans., 44 (2015) 10479-10489.
[38] J. Fujimoto, R. Okamoto, N. Noguchi, R. Hara, S. Masada, T. Kawamoto, H. Nagase, Y.O. Tamura, M. Imanishi, S. Takagahara, K. Kubo, K. Tohyama, K. Iida, T. Andou, I. Miyahisa, J. Matsui, R. Hayashi, T. Maekawa, N. Matsunaga, J. Med. Chem., 60 (2017) 8963-8981.
[39] S. Grimme, J. Comput. Chem., 27 (2006) 1787-1799.
[40] T. Ema, Y. Miyazaki, J. Shimonishi, C. Maeda, J.-Y. Hasegawa J. Am. Chem. Soc., 136 (2014) 15270-15279.

# The $CO_2$ cycloaddition to epoxides and aziridines promoted by porphyrin-based catalysts

Caterina Damiano[a], Paolo Sonzini[a], Matteo Cavalleri[a], Gabriele Manca[b]* and Emma Gallo[a]*

[a]Department of Chemistry, University of Milan, Via C. Golgi 19, 20133 Milan (Italy). E-mail: emma.gallo@unimi.it.

[b]Istituto di Chimica dei Composti OrganoMetallici, ICCOM-CNR, Via Madonna del Piano 10, I-50019 Sesto Fiorentino (Italy). E-mail: gabriele.manca@iccom.cnr.it

## TOC

The present short account reports our results on the catalytic activity of the $CO_2$ insertion into three-membered rings for the synthesis of valuable fine-chemicals. The DFT study of reaction mechanisms furnished important tools to improve performances of porphyrin-based catalytic procedures.